

Supplemental Table 1. The information of antibodies and kits

Name	Source	Product Number
p-p38	Cell Signaling	4511
p38 α	Cell Signaling	2371
p38 β	Cell Signaling	2339S
p-TAK1	Cell Signaling	9339
p-MKK3/6	Cell Signaling	12280S
p-IR	Cell Signaling	3024
IR β	Cell Signaling	23413
p-Akt	Cell Signaling	9271
p-FRS2 α	Cell Signaling	3864
Myc-tag	Cell Signaling	2276
HA-tag	Cell Signaling	3724
K48	Cell Signaling	8081
HSP90	Cell Signaling	4874S
p38	Abcam	ab27986
ubiquitin	Abcam	ab7780
KLB	Abcam	ab106794
MTTP	BD Pharmingen	612022
ApoB	Novus	NB200-527
KLB	Sigma	AV53325
Flag-tag	Sigma	F3165
TAK1	Proteintech	12330-2-AP
GAPDH	Proteintech	10494-1-AP
TRIM25	Abclonal	A19887
MKK6	Abclonal	A2575
LabAssay Triglyceride	Wako	290-63701
LabAssay NEFA	Wako	294-63601
Rat/Mouse Insulin ELISA Kit	Millipore	EZRMI-13K
Fibroblast Growth Factor 21	BioVender	RD291108200R
Mouse/Rat ELISA Phospho-p38 MAPK (Thr180/Tyr182) Sandwich ELISA Kit	CellSignaling	7946

Supplementary Table 2. Oligonucleotide sequences and reagents

Name	Sequence/Source	Note
MKK6-F	5'-GATTTAGACTCCAAGGCTTGC-3'	RT-PCR
MKK6-R	5'-TCCGCTTCACTGCCATGATCTG-3'	RT-PCR
p38 α -F	5'-ACAAGACCATCTGGGAGGTG-3'	RT-PCR
p38 α -R	5'-GTCCTTTTGGCGTGAATGAT-3'	RT-PCR
PPAR α -F	5'-GCGTACGGCAATGGCTTTAT-3'	RT-PCR
PPAR α -R	5'-GAACGGCTTCCTCAGGTTCTT-3'	RT-PCR
MCAD-F	5'-GCTCGTGAGCACaATTGAAAA-3'	RT-PCR
MCAD-R	5'-CATTGTCCAAAAGCCAAACC-3'	RT-PCR
CPT1 α -F	5'-AAAGATCAATCGGACCCTAGACA-3'	RT-PCR
CPT1 α -R	5'-CAGCGAGTAGCGCATAGTCA-3'	RT-PCR
CD36-F	5'-ATGGGCTGTGATCGGAACTG-3'	RT-PCR
CD36-R	5'-GTCTTCTCAATAAGCATGTCTCC-3'	RT-PCR
DGAT1-F	5'-TCCGTCCAGGGTGGTAGTG-3'	RT-PCR
DGAT1-R	5'-TGAACAAAGAATCTTGCAGACGA-3'	RT-PCR
DGAT2-F	5'-GCGCTACTTCCGAGACTACTT-3'	RT-PCR
DGAT2-R	5'-GGGCCTTATGCCAGGAAACT-3'	RT-PCR
GPAT-F	5'-GGCCTTCGGATTATCCCTGG-3'	RT-PCR
GPAT-R	5'-CTTGGGGGCTCCTTTCTGAA-3'	RT-PCR
ACSL1-F	5'-TGCCAGAGCTGATTGACATTC-3'	RT-PCR
ACSL1-R	5'-GGCATAACCAGAAGGTGGTGAG-3'	RT-PCR
MTPP-F	5'-CTCTTGGCAGTGCTTTTTCTCT-3'	RT-PCR
MTPP-R	5'-GAGCTTGTATAGCCGCTCATT -3'	RT-PCR
ApoB-F	5'-CCCCATCACTTTACAAGC-3'	RT-PCR
ApoB-R	5'-CAGAGCCATCAGGTAGGT-3'	RT-PCR
HSL-F	5'-TGTGGCACAGACCTCTAAAT-3'	RT-PCR
HSL-R	5'-GGCATATCCGCTCTC-3'	RT-PCR
ATGL-F	5'-GGAGACCAAGTGGAACATCTCA-3'	RT-PCR
ATGL-R	5'-AATAATGTTGGCACCTGCTTCA-3'	RT-PCR
FGF21-F	5'-TTGGGACCCTGGGACTGT-3'	RT-PCR
FGF21-R	5'-TGGCTGTTGGCAAAGAAA-3'	RT-PCR
XBP1s-F	5'-GGTCTGCTGAGTCCGCAGCAGG-3'	RT-PCR
XBP1s-R	5'-AGGCTTGGTGTATACATGG-3'	RT-PCR
XBP1t-F	5'-ACACGCTTGGGAATGGACAC-3'	RT-PCR
XBP1t-R	5'-CCATGGGAAGATGTTCTGGG-3'	RT-PCR
c-fos-F	5'-ACGCCGACTACGAGGCGTCA-3'	RT-PCR
c-fos-R	5'-CTGCGCAAAGTCCTGTGTGTTG-3'	RT-PCR
egr1-F	5'-GTCCTTTTCTGACATCGCTCTGA-3'	RT-PCR
egr1-R	5'-CGAGTCGTTTGGCTGGGATA-3'	RT-PCR
KLB-F	5'-ATCGGTTATGAAGGAATACA-3'	RT-PCR
KLB-R	5'-GTTTCAGTGCGTAGAAGTCG-3'	RT-PCR
TBP-F	5'-ACGGACAACCTGCGTTGATTT-3'	RT-PCR
TBP-R	5'-TTCTTGCTGCTAGTCTGGATTG-3'	RT-PCR
18s-F	5'-ACCGCAGCTAGGAATAATGGA-3'	RT-PCR

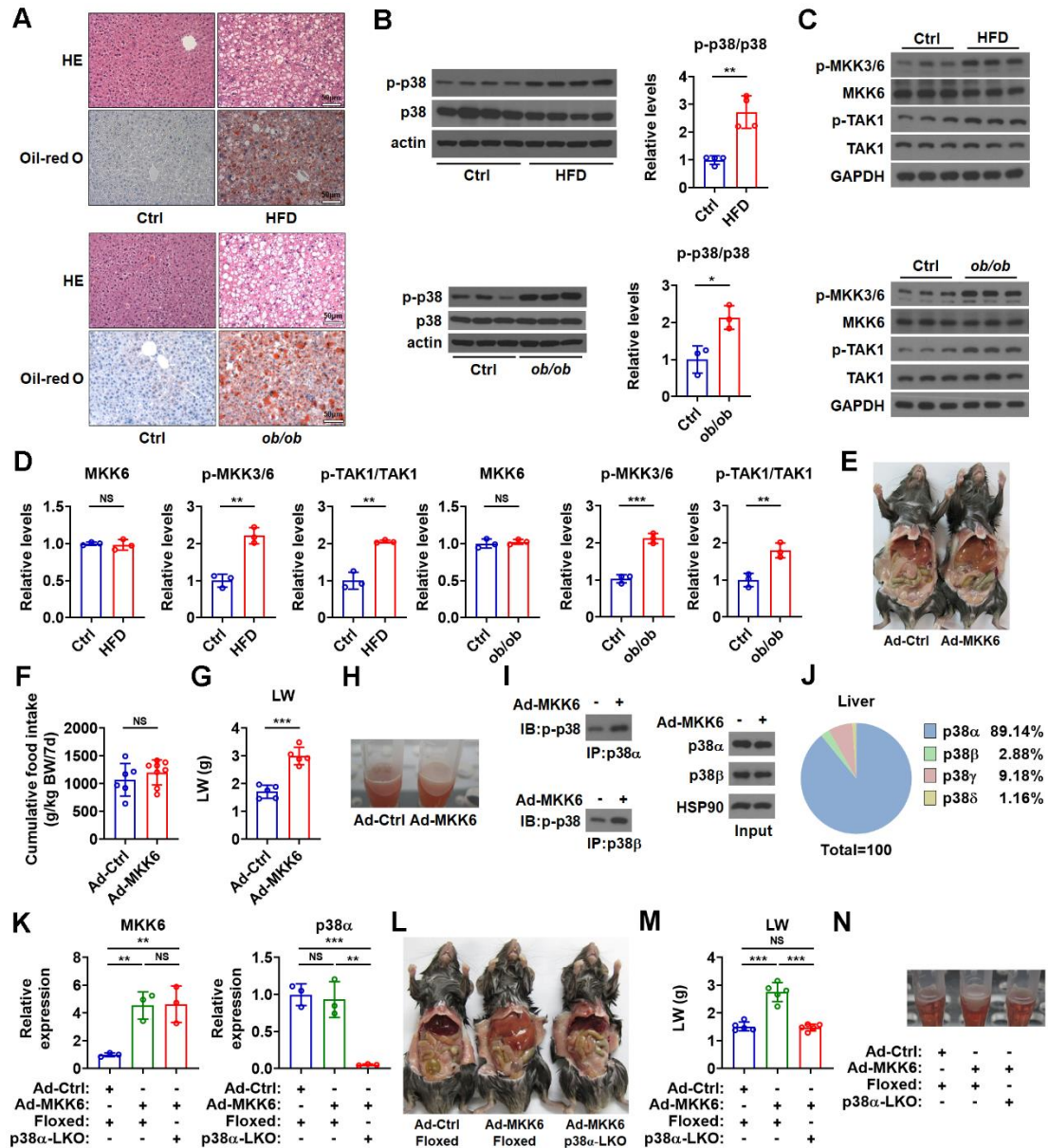
18s-R	5'-CAAATGCTTTCGCTCTGGTC-3'	RT-PCR
human FGF21-F	5'-ACCAGAGCCCCGAAAGTCT-3'	RT-PCR
human FGF21-R	5'-GACTCCCAAGATTTGAATAACTC-3'	RT-PCR
human KLB-F	5'-TTCTGGGGTATTGGGACTGGA-3'	RT-PCR
human KLB-R	5'-CCATTCGTGCTGCTGACATTTT-3'	RT-PCR
xbp1s-F	5'-ACACGCTTGGGAATGGACAC-3'	PCR and electrophoresis
xbp1s-R	5'-CCATGGGAAGATGTTCTGGG-3'	PCR and electrophoresis
sgRNA-lacZ	5'-TGCGAATACGCCACGCGAT-3'	p38 α ko HEK293T cell
sgRNA-p38 α	5'-TACCAGAACCTGTCTCCAGT-3'	p38 α ko HEK293T cell
mutation test690-F	5'-CCCGTTTGCTGGCTCTTGGA-3'	PCR and electrophoresis
mutation test690-R	5'-TGGACCGCATACCTGCGTGA-3'	PCR and electrophoresis
siZNF598-1-F	5'-GACAAUGAUGAGCUGCUUAAGTT-3'	siRNA
siZNF598-1-R	5'-CUUAAGCAGCUCAUCAUUGUCTT-3'	siRNA
siZNF598-2-F	5'-GAUGGAAAGGUGUACGCAUUGTT-3'	siRNA
siZNF598-2-R	5'-CAAUGCGUACACCUUCCAUCTT-3'	siRNA
siZNF598-3-F	5'-CCUCGACAAAUGGUCCUGUAATT-3'	siRNA
siZNF598-3-R	5'-UUACAGGACCAUUUGUCGAGGTT-3'	siRNA
siTRIM25-1-F	5'-CCGGAACAGUUAGUGGAUUUATT-3'	siRNA
siTRIM25-1-R	5'-UAAAUCCACUAACUGUCCGGTT-3'	siRNA
siTRIM25-2-F	5'-ACAACAAGAAUACACGGAAAUTT-3'	siRNA
siTRIM25-2-R	5'-AUUUCGUGUAUUCUUGUUGUTT-3'	siRNA
siTRIM25-3-F	5'-GAGUGAGAUCAGACCUUGAATT-3'	siRNA
siTRIM25-3-R	5'-UUCAAGGUCUGGAUCUCACUCTT-3'	siRNA
siMKRN2-1-F	5'-UUGGUUCUUAGAGACCGAAAUTT-3'	siRNA
siMKRN2-1-R	5'-AUUUCGGUCUCUAAGAACCAATT-3'	siRNA
siMKRN2-2-F	5'-UGGGUGGAAGAUCAGAAUAAATT-3'	siRNA
siMKRN2-2-R	5'-UUUAUUCUGAUCUCCACCCATT-3'	siRNA
siMKRN2-3-F	5'-GACCUCUUCAUGCACCUUUCUTT-3'	siRNA
siMKRN2-3-R	5'-AGAAAGGUGCAUGAAGAGGUUCTT-3'	siRNA
siCHIP-1-F	5'-GCAGUCUGUGAAGGCGCACUUTT-3'	siRNA
siCHIP-1-R	5'-AAGUGCGCCUUCACAGACUGCTT-3'	siRNA
siCHIP-2-F	5'-CGCGAAGAAGAAGCGCUGGAATT-3'	siRNA
siCHIP-2-R	5'-UCCAGCGCUUCUUCUUCGCGTT-3'	siRNA
siCHIP-3-F	5'-GAAGAGGAAGAAGCGAGACAUTT-3'	siRNA
siCHIP-3-R	5'-AUGUCUCGCUUCUCCUCUUCTT-3'	siRNA
p38 α -F	5'-ATGTCTCAGGAGAGGCCACGTT-3'	plasmid
p38 α -R	5'-TCAGGACTCCATCTCTTCTTGGTC-3'	plasmid
TRIM25-F	5'-ATGGCAGAGCTGTGCCCCCTGGC-3'	plasmid

TRIM25-R	5'-TACTTGGGGGAGCAGATGGAGAG-3'	plasmid
MKK6-F	5'-ATGTCTCAGTCGAAAGGCAA-3'	adenovirus and plasmid
MKK6-R	5'-TTAGTCTCCAAGAATCAGTT-3'	adenovirus and plasmid
FGF21-F	5'-ACAGCCATTCACCTTTGCC-3'	adenovirus
FGF21-R	5'-CAGCCCTAGATTCAGGAAGA-3'	adenovirus
shKLB-1014T	5'-CACCGCGACTACCCTGAGTTCATGA CGAATCATGAACTCAGGGTAGTCGC-3'	shRNA knockdown
shKLB-1014B	5'-AAAAGCGACTACCCTGAGTTCATGA TTCGTCATGAACTCAGGGTAGTCGC-3'	shRNA knockdown
FGF21-pro-F	5'-ACAGATTAAGCCACCGAGTC-3'	Promoter
FGF21-pro-R	5'-TCTGGTGAACGCAGAAATAC-3'	Promoter
p38 α Floxed-F	5'-TCCTACGAGCGTCGGCAAGGTG-3'	Genotyping
p38 α Floxed-R	5'-AGTCCCCGAGAGTTCCTGCCTC-3'	Genotyping
FGF21 Floxed-F	5'-GACCCTGTCATTCCCCACT-3'	Genotyping
FGF21 Floxed-R	5'-TGCTTGTCCAGGTTTGAG-3'	Genotyping
Alb-cre-F	5'-GGTCGATGCAACGAGTGATGAGG-3'	Genotyping
Alb-cre-R	5'-CCAGAGACGGAAATCCATCGCTCG- 3'	Genotyping
LysM-cre-F	5'-CCCAGAAATGCCAGATTACG-3'	Genotyping
LysM-cre-R	5'-CTTGGGCTGCCAGAATTTCTC-3'	Genotyping
Anisomycin	MedChemExpress	HY-18982
Cycloheximide	MedChemExpress	HY-12330
MG132	MedChemExpress	HY-13259
Chloroquine	MedChemExpress	HY-17589A
Bafilomycin A1	MedChemExpress	HY-100558

Supplemental Table 3. The information of human subjects

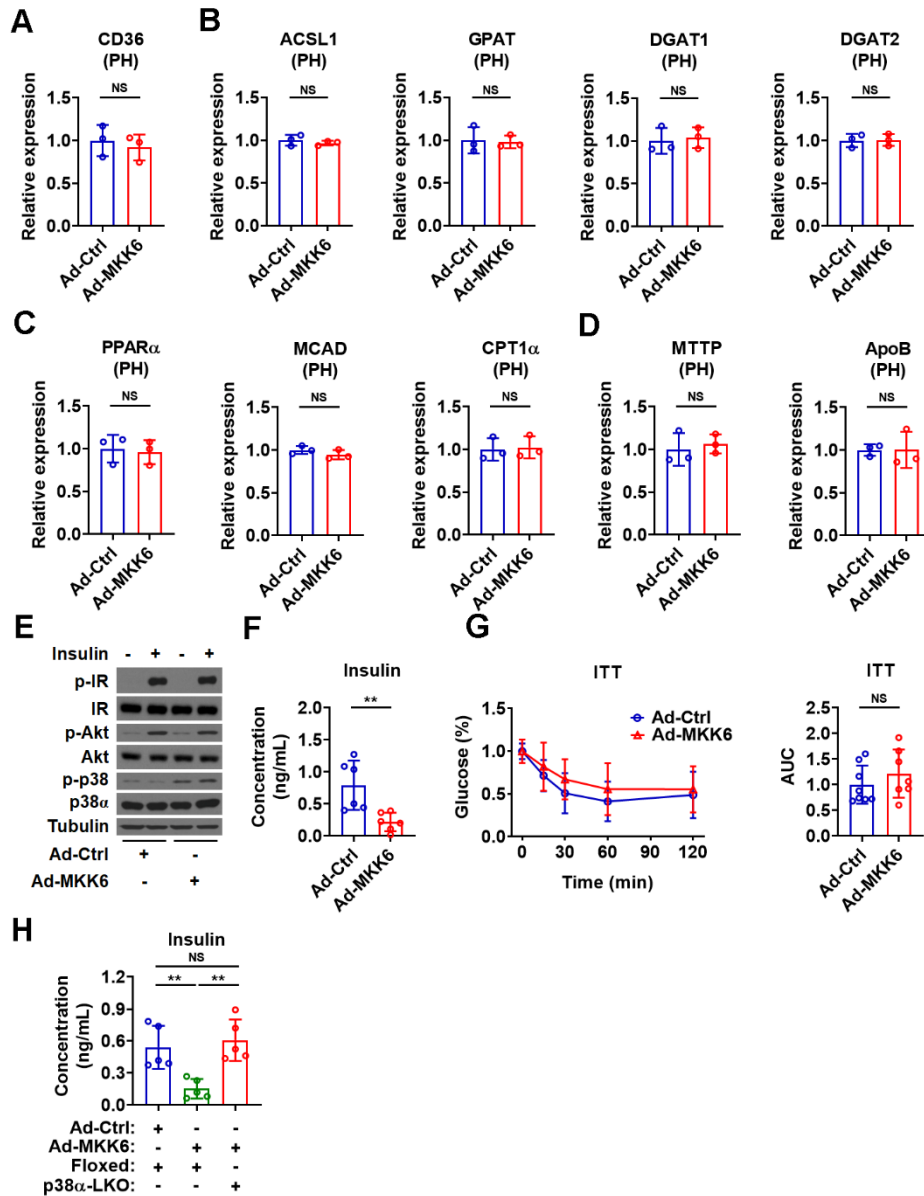
liver	Gender (F/M)	Age (Yr)	Bw (kg)	Height (cm)	BMI (kg/m ²)	ALT (U/L)	AST (U/L)
Normal	F	64	51	167	18.29	25	30
Normal	M	44	80	178	25.25	36	21
Normal	F	38	53	171	18.13	7	15
Normal	F	50	61	167	21.87	14	19
Normal	F	31	43	156	17.67	13	20
Fatty	M	39	138	170	47.75	28	19
Fatty	F	44	139.7	170	48.34	44	33
Fatty	F	32	98.2	156	40.35	46	31
Fatty	F	64	96.1	159	38.01	42	22
Fatty	F	34	129.8	185	37.93	127	121

Supplementary figures and figure legends



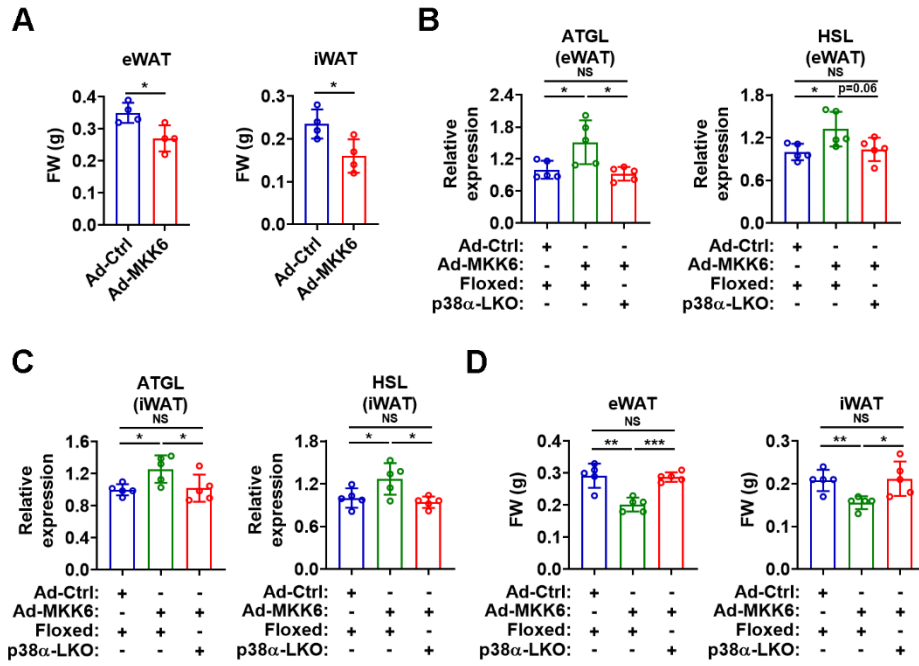
Supplemental Figure 1. Hepatic p38 is activated in fatty liver and its activation by Ad-MKK6 results in severe liver steatosis.

(A-D) H&E and Oil-red O staining of liver sections (A), western blots and densitometry analysis (B-D) of p-p38, MKK6, p-MKK3/6, and p-TAK1 in the liver of HFD and *ob/ob* mice and their corresponding control mice as indicated (n=3-4). (E-H) Internal organs (E) (liver, eWAT, etc.), cumulative food intake (F, n=6-8), liver weight (LW) (G, n=5), lipid layer of the liver lysates (H) of mice infected with Ad-MKK6. (I) IP and IB analysis with indicated antibodies after HepG2 cells were treated with Ad-MKK6. (J) Absolute-quantification of p38 isoforms in mouse liver by RT-PCR and the relative proportion of each p38 isoforms is shown (n=5). (K) qRT-PCR analysis of MKK6 (left) and p38 α (right) in the liver of p38 α -LKO mice infected with Ad-MKK6 (n=3). (L and M) Internal organs (liver, eWAT, etc.) (L) and LW (M, n=5) of p38 α -LKO mice infected with Ad-MKK6. (N) Lipid layer of the liver lysates of p38 α -LKO mice infected with Ad-MKK6 after centrifugation. Means \pm SD are shown. * p <0.05; ** p <0.01; *** p <0.001; NS, not significant.



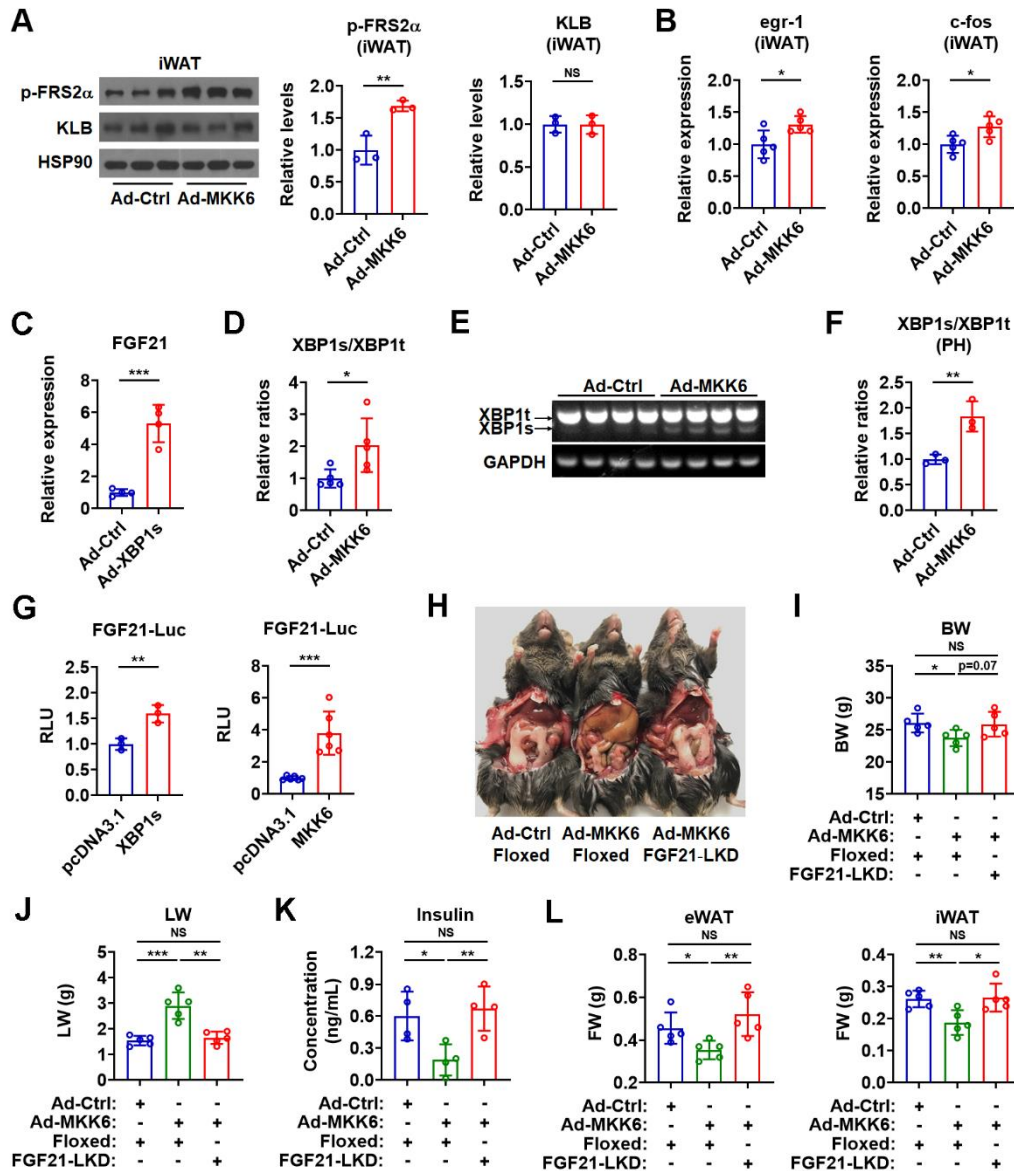
Supplemental Figure 2. Hepatic p38 activation acts non-cell-autonomously to modulate the metabolism.

(A and B) qRT-PCR analysis of CD36 (A), ACSL1, GPAT, DGAT1, and DGAT2 (B) in primary hepatocytes infected with Ad-MKK6 (n=3). (C and D) qRT-PCR analysis of PPAR α , MCAD, CPT1 α (C), MTP, and ApoB (D) in the primary hepatocytes infected with Ad-MKK6 (n=3). (E) Western blot analysis of p-p38, p-IR and p-Akt in the primary hepatocytes infected with Ad-MKK6 after insulin administration. (F) Serum insulin levels in the mice infected with Ad-MKK6 (n=6). (G) Insulin-tolerance test (ITT) was performed in mice infected with Ad-MKK6 (n=7-8). Area under the curve (AUC) for ITT was calculated. (H) Serum insulin levels of p38 α -LKO mice infected with Ad-MKK6 (n=5). Means \pm SD are shown. ** p <0.01; NS, not significant.



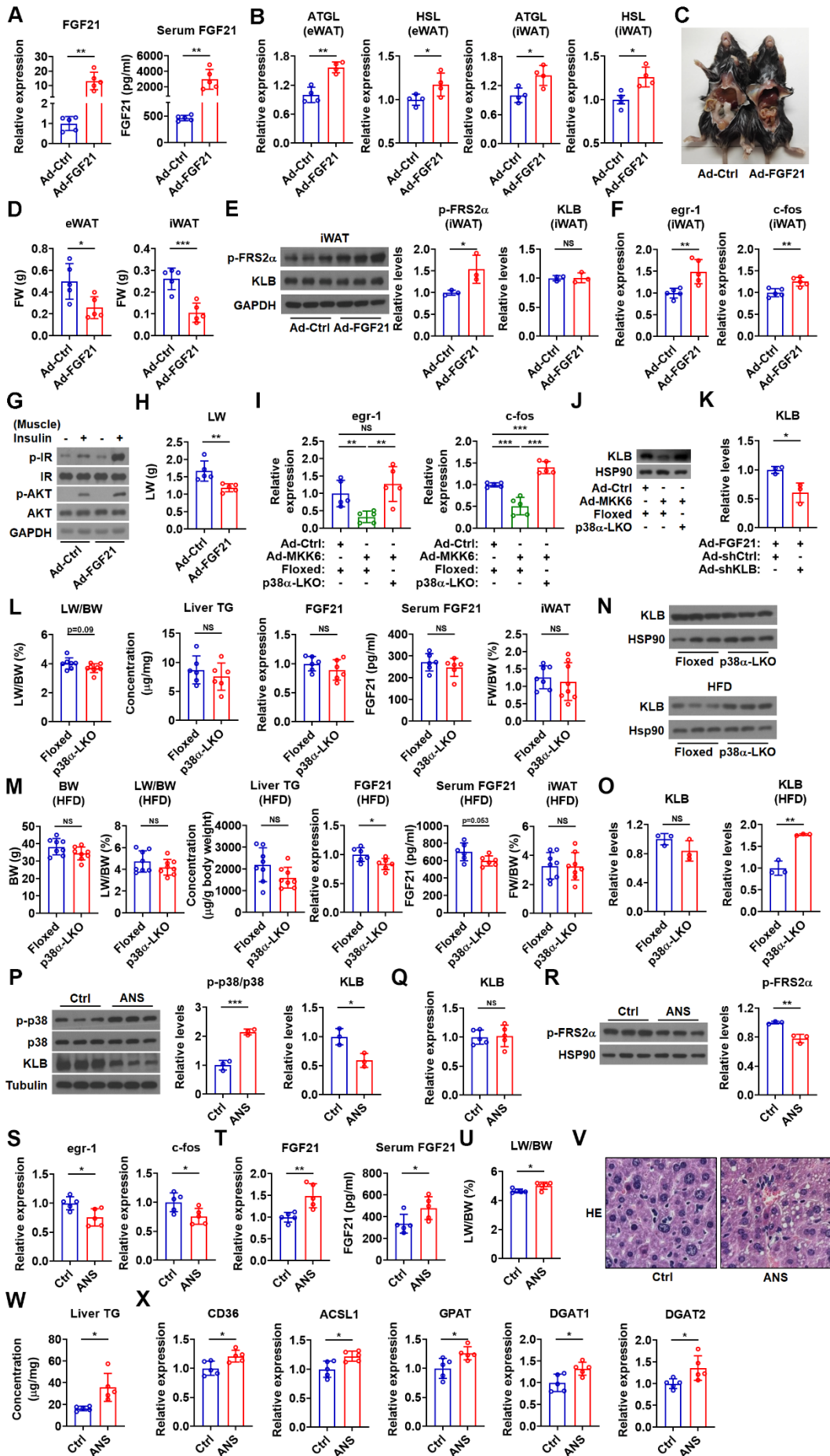
Supplemental Figure 3. Hepatic p38 activation by Ad-MKK6 enhances the lipolysis in WATs.

(A) Weight of eWAT (left) and iWAT (right) in mice infected with Ad-MKK6 (n=4). (B) qRT-PCR analysis of ATGL (left) and HSL (right) in the eWAT of p38 α -LKO mice infected with Ad-MKK6 (n=5). (C) qRT-PCR analysis of ATGL (left) and HSL (right) in the iWAT of p38 α -LKO mice infected with Ad-MKK6 (n=5). (D) Weight of eWAT (left) and iWAT (right) in p38 α -LKO mice infected with Ad-MKK6 (n=5). Means \pm SD are shown. * p <0.05; ** p <0.01; *** p <0.001; NS, not significant.



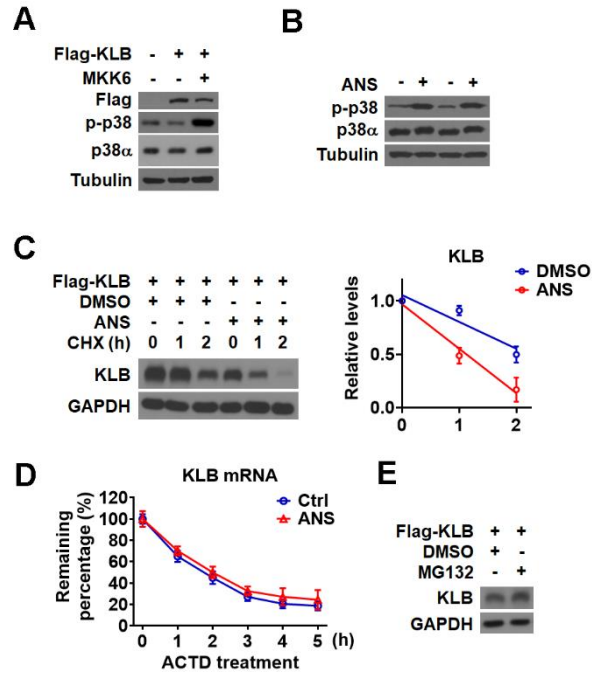
Supplemental Figure 4. Liver-derived FGF21 mediates the metabolic effects of hepatic p38 activation.

(A) Western blot and densitometry analysis of p-FRS2 α and KLB levels in the iWAT of mice infected with Ad-MKK6 (n=3). (B) Relative egr-1 and c-fos mRNA levels in the iWAT of mice infected with Ad-MKK6 (n=5). (C) Relative FGF21 mRNA levels in the liver of mice infected with Ad-XBP1s (n=4). (D) Relative XBP1s/XBP1t mRNA ratios in the liver of mice infected with Ad-MKK6 (n=5). (E) RT-PCR analysis of the mRNA levels of XBP1s and XBP1t by agarose gel electrophoresis using a single pair of primers in the liver of mice infected with Ad-MKK6 (n=4). (F) Relative XBP1s/XBP1t mRNA ratios in the primary hepatocytes infected with Ad-MKK6 (n=4). (G) Activity of the reporter containing FGF21 promoter in HEK293T cells transfected with XBP1s (left, n=3) or MKK6 (right, n=6). (H) Internal organs (liver, eWAT, etc.) of FGF21-LKD mice infected with Ad-MKK6. (I and J) BW (I) and LW (J) of FGF21-LKD mice infected with Ad-MKK6 (n=5). (K) Serum insulin levels of FGF21-LKD mice infected with Ad-MKK6 (n=4). (L) Weight of eWAT and iWAT in FGF21-LKD mice infected with Ad-MKK6 (n=5). Means \pm SD are shown. *p<0.05; **p<0.01; ***p<0.001; NS, not significant.



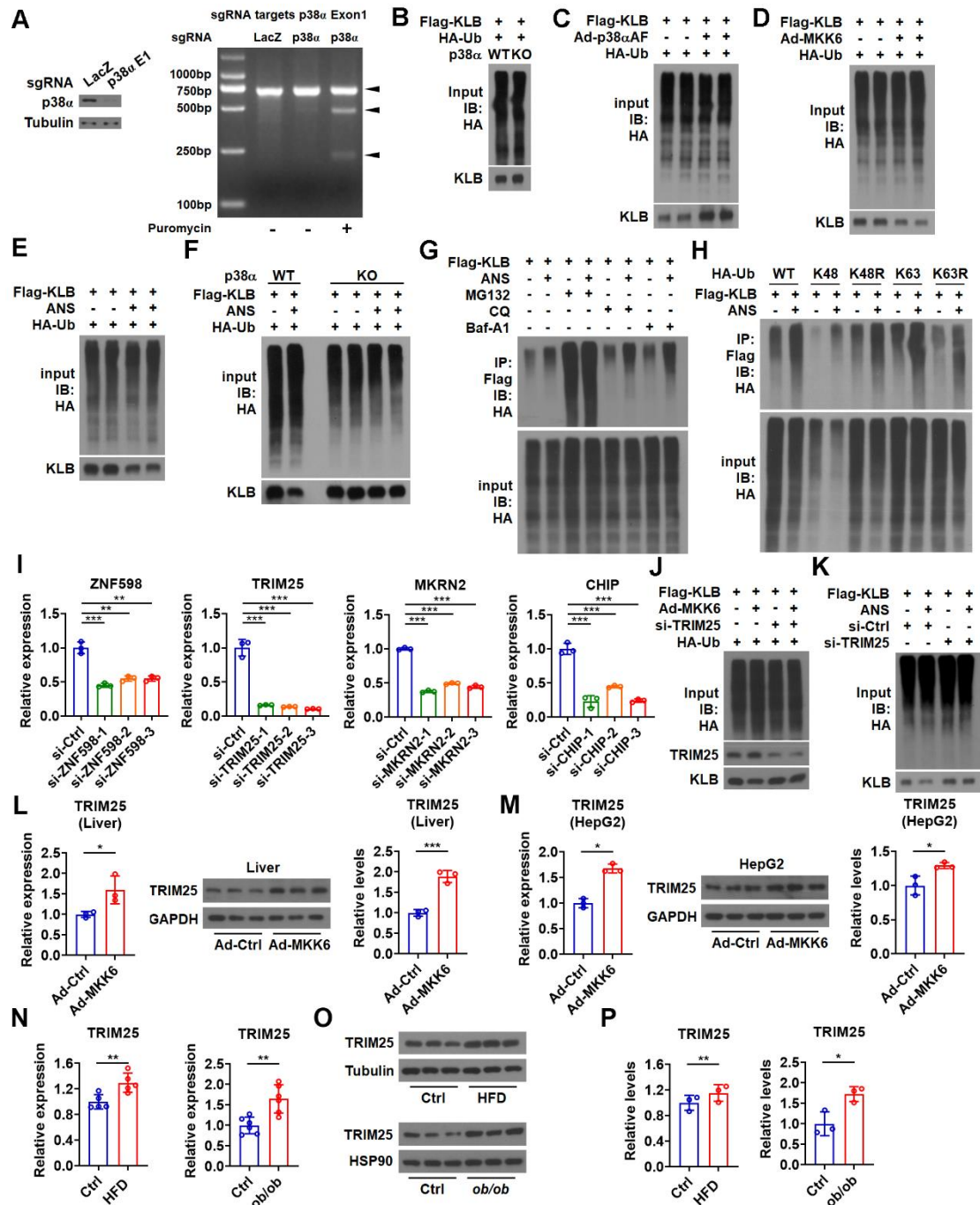
Supplemental Figure 5. Activation of hepatic p38 attenuates the local FGF21 action in liver.

(A) Relative FGF21 mRNA levels in the liver (left) and serum FGF21 levels (right) of mice infected with Ad-FGF21 (n=5). (B) Relative mRNA levels of ATGL and HSL in the eWAT and iWAT of mice infected with Ad-FGF21 as indicated (n=4). (C) Internal organs (liver, eWAT, etc.) of mice infected with Ad-FGF21. (D) Weight of eWAT and iWAT of mice infected with Ad-FGF21 (n=5). (E) Western blot and densitometry analysis of p-FRS2 α and KLB levels in the iWAT of mice infected with Ad-FGF21 (n=3). (F) Relative egr-1 and c-fos mRNA levels in the iWAT of mice infected with Ad-FGF21 (n=5). (G) Western blot analysis of insulin-induced phosphorylation of IR and Akt in the skeletal muscle of mice infected with Ad-FGF21. (H) Liver weight (LW) of mice infected with Ad-FGF21 (n=5). (I) qRT-PCR analysis of egr-1 and c-fos in the liver of p38 α -LKO mice infected with Ad-MKK6 as indicated (n=5). (J) Western blot analysis of KLB in the liver of p38 α -LKO mice and control Floxed mice infected with Ad-MKK6 as indicated. (K) Densitometry analysis of KLB for the western blot shown in Figure 5O (n=3). (L) LW/BW, liver TG, relative FGF21 mRNA levels in the liver, serum FGF21 levels and ratios of iWAT weights to BW of p38 α -LKO and control Floxed mice (n=6-8). (M) BW, LW/BW, liver TG, relative FGF21 mRNA levels in the liver, serum FGF21 levels and ratios of iWAT weights to BW of p38 α -LKO and control Floxed mice on HFD (n=6-8). (N and O) Western blot (N) and densitometry (O) analysis of KLB in the liver of p38 α -LKO mice and control Floxed mice on normal chow diet and HFD (n=3). (P) Western blot and densitometry analysis of p-p38 and KLB in the liver of mice treated with ANS (n=3). (Q) Relative mRNA levels of KLB in the liver of mice treated with ANS (n=5). (R) Western blot and densitometry analysis of p-FRS2 α in the liver of mice treated with ANS (n=3). (S) Relative mRNA levels of egr-1 and c-fos in the liver of mice treated with ANS (n=5). (T) Relative FGF21 mRNA levels in the liver (left) and serum FGF21 levels (right) of mice treated with ANS (n=5). (U-W) LW/BW (U), representative images of H&E staining (V) of liver sections and liver TG levels (W) of mice treated with ANS. (X) Relative CD36, ACSL1, GPAT, DGAT1 and DGAT2 mRNA levels in the liver of mice treated with ANS (n=5). Means \pm SD are shown. *p<0.05; **p<0.01; ***p<0.001; NS, not significant.



Supplemental Figure 6. Activation of p38 facilitates the degradation of KLB.

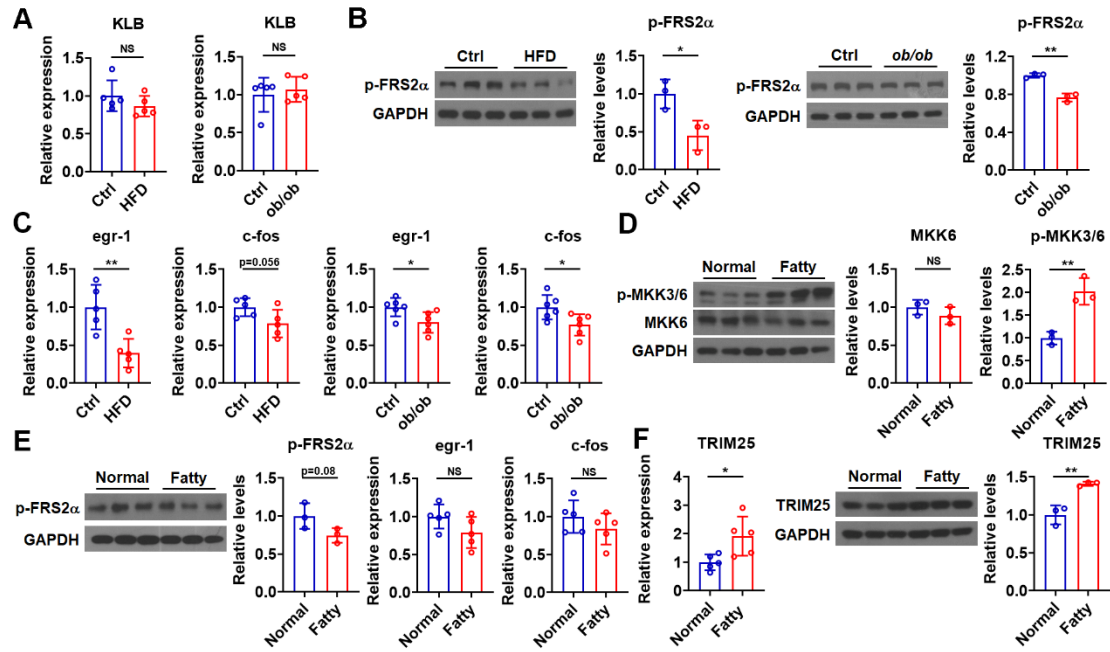
(A) Western blot analysis of Flag-KLB and p-p38 in HEK293T cells transfected with indicated plasmids. (B) Western blot analysis of p-p38 in HEK293T cells treated with ANS. (C) Western blot (left) and linear regression (right) analysis of the rate of decay of Flag-KLB in Flag-KLB-transfected HEK293T cells treated with ANS in the presence of CHX for indicated time periods. (D) Remaining Flag-KLB mRNA in Flag-KLB-transfected HEK293T cells at different time points after ANS treatment in the presence of Actinomycin D (ACTD). (E) Western Blot analysis of KLB in HEK293T cells transfected with Flag-KLB for 12 h and then treated with MG132 for 12 h. Means \pm SD are shown.



Supplemental Figure 7. Activation of p38 promotes ubiquitination of KLB through TRIM25.

(A) Western blot analysis of p38 α (left) and analysis of the cleavage efficiency of Cas9-mediated cleavage of p38 α locus (right) in Cas9-expressing HEK293T cells transfected with either LacZ-targeting sgRNA or p38 α -targeting sgRNA after puromycin selection. (B) p38 α WT and KO cells were transfected with the plasmids, followed by IB analysis with indicated antibodies. (C, D, and E) HEK293T cells were transfected with plasmids and infected with Ad-p38 α AF (C) or Ad-MKK6 (D), or treated with ANS (E), followed by IB analysis with indicated antibodies. (F) p38 α WT and KO cells were transfected with plasmids and treated with ANS, followed by IB analysis with indicated antibodies. (G) IP and IB analysis with indicated antibodies after HEK293T cells were transfected with indicated plasmids and then treated with MG132, CQ and Baf-A1. (H) IP and IB analysis with indicated antibodies after HEK293T cells were transfected with indicated plasmids

and then treated with ANS. (I) HEK293T cells were transfected with indicated siRNA and then the mRNA levels of each gene were analyzed. (J and K) IB analysis after Flag-KLB-transfected HEK293T cells were transfected with indicated siRNA and then infected with Ad-MKK6 (J) or treated with ANS (K). A pool of three siRNAs targeting different regions of TRIM25 was used. (L and M) qRT-PCR and western blot analysis of TRIM25 in the liver of mice (L) or HepG2 cells (M) infected with Ad-MKK6 (n=3). (N-P) qRT-PCR (N, n=5), western blot (O) and densitometry (P) analysis of TRIM25 in the liver of HFD and *ob/ob* mice. Means \pm SD are shown. * $p < 0.05$; ** $p < 0.01$; *** $p < 0.001$.



Supplemental Figure 8. KLB mRNA levels in the fatty liver of mice.

(A) qRT-PCR analysis of KLB in the liver of HFD and *ob/ob* mice (n=5). (B) Western blot and densitometry analysis of p-FRS2 α in the liver of HFD and *ob/ob* mice (n=3). (C) qRT-PCR analysis of egr-1 and c-fos in the liver of HFD and *ob/ob* mice (n=5). (D) Western blots and densitometry analysis of p-MKK3/6 and MKK6 in the liver of human subjects with normal or fatty liver (n=3). (E) Western blot and densitometry analysis of p-FRS2 α and qRT-PCR analysis of egr-1 and c-fos in the liver of human subjects with normal or fatty liver (n=3). (F) qRT-PCR analysis (n=5) and western blot and densitometry analysis (n=3) of TRIM25 in the liver of human subjects with normal or fatty liver. Means \pm SD are shown. NS, not significant. * $p<0.05$; ** $p<0.01$; NS, not significant.